

Lattice field theory results for hybrid static potentials at short quark-antiquark separations and their parametrization

Carolin Schlosser,^{a,b,*} Sonja Köhler^a and Marc Wagner^{a,b}

^a*Institut für Theoretische Physik, Goethe-Universität Frankfurt am Main,
Max-von-Laue-Straße 1, D-60438 Frankfurt am Main, Germany*

^b*Helmholtz Research Academy Hesse for FAIR, Campus Riedberg,
Max-von-Laue-Straße 12, D-60438 Frankfurt am Main, Germany*

*E-mail: schlosser@itp.uni-frankfurt.de, skoehler@itp.uni-frankfurt.de,
mwagner@itp.uni-frankfurt.de*

We present SU(3) lattice Yang-Mills data for hybrid static potentials from five ensembles with different small lattice spacings and the corresponding parametrizations for quark-antiquark separations $0.08 \text{ fm} \leq r \leq 1.12 \text{ fm}$. We remove lattice discretization errors at tree level of perturbation theory and partly at order a^2 as well as the a -dependent self energy. In particular the tree-level improvement of static potentials is discussed in detail and two methods are compared. The resulting parametrizations are expected to represent continuum limit results for hybrid static potentials within statistical errors.

*The 39th International Symposium on Lattice Field Theory,
8th-13th August, 2022,
Rheinische Friedrich-Wilhelms-Universität Bonn, Bonn, Germany*

*Speaker

1. Introduction

The goal of our work is to compute precise results for the hybrid static potentials Π_u and Σ_u^- at short quark-antiquark separations using SU(3) lattice Yang-Mills theory. The hybrid static potentials Π_u and Σ_u^- describe the two lowest excitations of the gluon field surrounding a static quark-antiquark pair as a function of the quark-antiquark separation. For the related heavy hybrid mesons, exotic quantum number combinations J^{PC} are possible due to the non-trivial quantum numbers of the gluonic excitation. They are – like tetraquarks and glueballs – an active field of research in experiments as well as in theory (for recent reviews see e.g. [1–6]). Lattice field theory results for hybrid static potentials are an essential input for mass calculations of heavy $\bar{b}b$ or $\bar{c}c$ hybrid mesons within the Born-Oppenheimer approximation [7–11]. Refined Born-Oppenheimer approaches also include heavy quark spin effects or the coupling of different channels [12–14].

For reliable predictions of heavy hybrid meson masses within such approaches precise lattice field theory results and parametrizations for the corresponding static potentials are important. To improve on existing lattice field theory computations of hybrid static potentials [7, 11, 15–21], we use lattice spacings significantly smaller than those used in existing works. This allows us to remove lattice discretization errors at tree level of perturbation theory and to some extent at leading order in a^2 . We obtain improved lattice results and parametrizations consistent with continuum limit results for the hybrid static potentials Π_u and Σ_u^- within statistical errors.

2. Lattice setup

We generated five ensembles of pure SU(3) gauge field configurations with the CL2QCD software package [22] using a Monte Carlo heatbath algorithm and the standard Wilson plaquette action. The ensembles *A*, *B*, *C* and *D* (listed in Table 1) were generated with gauge couplings $\beta = 6.000, 6.284, 6.451$ and 6.594 , which correspond to lattice spacings $a = 0.093$ fm, 0.060 fm, 0.048 fm and 0.040 fm, respectively. The scale is set according to a parametrization of $\ln(a/r_0)$ from Ref. [23] and by identifying r_0 with 0.5 fm. To achieve a reduction of statistical errors, a multilevel algorithm [24] was used on ensembles *A*, *B*, *C* and *D*. We confirmed that finite volume effects are negligible for the physical lattice volumes of ensembles *A*, *B*, *C* and *D*, which are $T \times L^3 \approx 2.4$ fm \times $(1.2$ fm) 3 . Moreover, we checked that the measurements are neither affected by large autocorrelations nor topology freezing. For details on the exclusion

ensemble	β	a in fm [23]	$(L/a)^3 \times T/a$
<i>A</i>	6.000	0.093	$12^3 \times 26$
<i>B</i>	6.284	0.060	$20^3 \times 40$
<i>C</i>	6.451	0.048	$26^3 \times 50$
<i>D</i>	6.594	0.040	$30^3 \times 60$
A^{HYP2}	6.000	0.093	$24^3 \times 48$

Table 1: Gauge link ensembles.

of systematic errors from the finite volume, topology and also possible decays into glueballs see Ref. [25].

We also include lattice results from ensemble A^{HYP2} , which were obtained in the context of a preceding project and publication [11]. The lattice spacing is the same as for ensemble A but, due to the larger lattice volume, larger quark-antiquark separations up to $r \leq 1.12$ fm were accessible. In contrast to results from ensembles A , B , C and D , results from ensemble A^{HYP2} were computed with HYP2-smearred temporal links [26–28], which reduces the self energy of the static quarks but increases discretization errors at small r/a .

3. Lattice field theory computation of (hybrid) static potentials

We compute hybrid static potentials from Wilson loop-like correlation functions on the five ensembles $e \in \{A, B, C, D, A^{\text{HYP2}}\}$. In contrast to standard Wilson loops related to the ordinary static potential with quantum numbers $\Lambda_{\eta}^{\epsilon} = \Sigma_g^+$, the spatial link paths of the hybrid Wilson loops include suitable insertions to generate the non-trivial quantum numbers of hybrid static potentials. The quantum numbers $\Lambda_{\eta}^{\epsilon}$ denote the orbital angular momentum along the quark-antiquark separation axis, $\Lambda = \Sigma (= 0), \Pi (= 1), \Delta (= 2), \dots$, the behavior under combined parity and charge conjugation, $\eta = g (= +), u (= -)$, and the behavior under reflection along an axis orthogonal to the quark separation axis, $\epsilon = +, -$. To compute the potentials Π_u and Σ_u^- , we use the insertions $S_{\text{III},1}$ and $S_{\text{IV},2}$, which were defined and optimized for maximal ground state overlaps in Ref. [11]. To further increase the ground state overlaps, spatial links are smeared with APE-smearing on all ensembles with $\alpha_{\text{APE}} = 0.5$, where the number of smearing steps N_{APE} was increased with decreasing lattice spacing (see Ref. [25] for details).

The static potentials $aV_{\Lambda_{\eta}^{\epsilon}}^e(r)$ are extracted by plateau fits of the corresponding effective potentials at large temporal separations of the Wilson loops. Our SU(3) lattice Yang-Mills theory results for the ordinary static potential and the two lowest hybrid static potentials are presented in Figure 1. To show the lattice data from all ensembles together in a meaningful plot in Figure 1, we set $V_{\Sigma_g^+}^e(r = 0.5r_0) = 0$ for $e \in \{A, B, C, D, A^{\text{HYP2}}\}$ to compensate for the ensemble-dependent self energy of the static quarks.

At our level of statistical precision, lattice discretization errors lead to large discrepancies between lattice results from different ensembles covering the same range of physical quark-antiquark separations. This is visualized in Figure 2 for the ordinary static potential. In the following section 4 we discuss how to remove discretization errors to a large extent. After that, in section 5, we are able to provide a common parametrization of all available lattice data sets representing their continuum limit.

4. Comparison of two methods of tree-level improvement for the static potential

We now discuss and compare two commonly used methods (in the following referred to as r -method and V -method) to reduce lattice discretization errors for the static potential at tree level of perturbation theory. To assess the effectiveness of both methods, we plot lattice field theory data for the ordinary static potential for gauge group SU(2) at gauge coupling $\beta = 2.40$ computed with

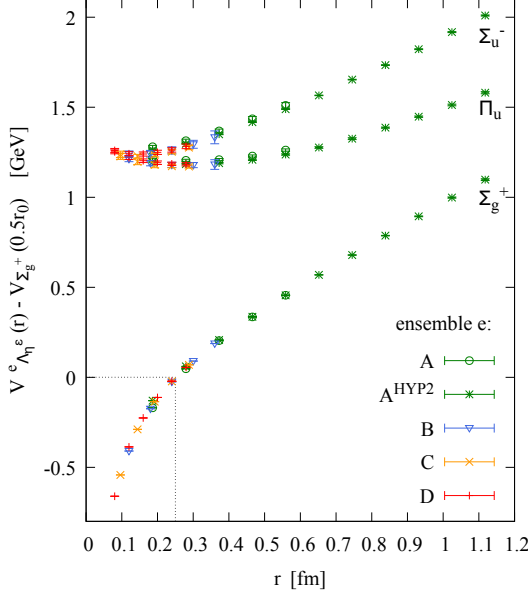


Figure 1: SU(3) lattice field theory results for the ordinary static potential Σ_g^+ and the hybrid static potentials Π_u and Σ_u^- from the five ensembles $e \in \{A, B, C, D, A^{\text{HYP2}}\}$.

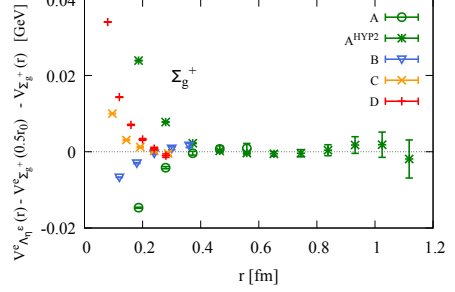


Figure 2: Visualization of lattice discretization errors in the lattice data for Σ_g^+ . $V^e_{\Sigma_g^+}(r)$ as defined in Eq. (3) is subtracted from the data shown in Figure 1.

two different discretizations of the static action, the HYP2 static action and the standard Eichten-Hill static action. The two discretizations should lead to similar results, where discrepancies are the consequence of lattice discretization errors. For the unimproved data shown in Figure 3a, discretization errors are rather large, particularly pronounced at small r/a . These errors also cause a breaking of rotational symmetry, which is reflected by the discrepancy of data points from on-axis Wilson loops and from off-axis Wilson loops with the same spatial separation, e.g. $r/a = |\mathbf{r}|/a = 3$ with $\mathbf{r}/a = (3, 0, 0)$ and $\mathbf{r}/a = (2, 2, 1)$.

The r -method of improvement was introduced for the static force [29]. The basic idea is to match the static force computed on the lattice at tree level of perturbation theory with the corresponding continuum result. Later, the r -method was also adopted for the static potential [23]. A static potential data point is shifted from its original separation r to an improved separation r_{impr} defined via $(4\pi r_{\text{impr}})^{-1} = G(\mathbf{r}/a)/a$, where $G(\mathbf{r}/a)$ represents the lattice propagator at tree level, which depends on the discretization of the static action. The resulting improved data is presented in Figure 3b. There is still a sizable discrepancy resulting from an overcorrection of data points. A universal parametrization of the two lattice data sets with small $\chi^2/\text{dof} \approx 1$ is not possible.

One can try to cope with the remaining discretization errors, e.g. by adding systematic errors to data points at small r to reduce their weight in subsequent fits or by multiplying the data with a correction factor [30–33]. We have explored a different strategy. First we have checked that the overcorrection can be consistently described by $\bar{\Delta}^{\text{lat}} = \sigma(r - r_{\text{impr}})$, where σ denotes a fit parameter closely related to the string tension. This expression can be motivated by noting that a Cornell ansatz $V_0 - \alpha/r + \sigma r$ is a reasonable description of the ordinary static potential and by assuming that one-gluon exchange is strongly related to the α/r term, but not to the other

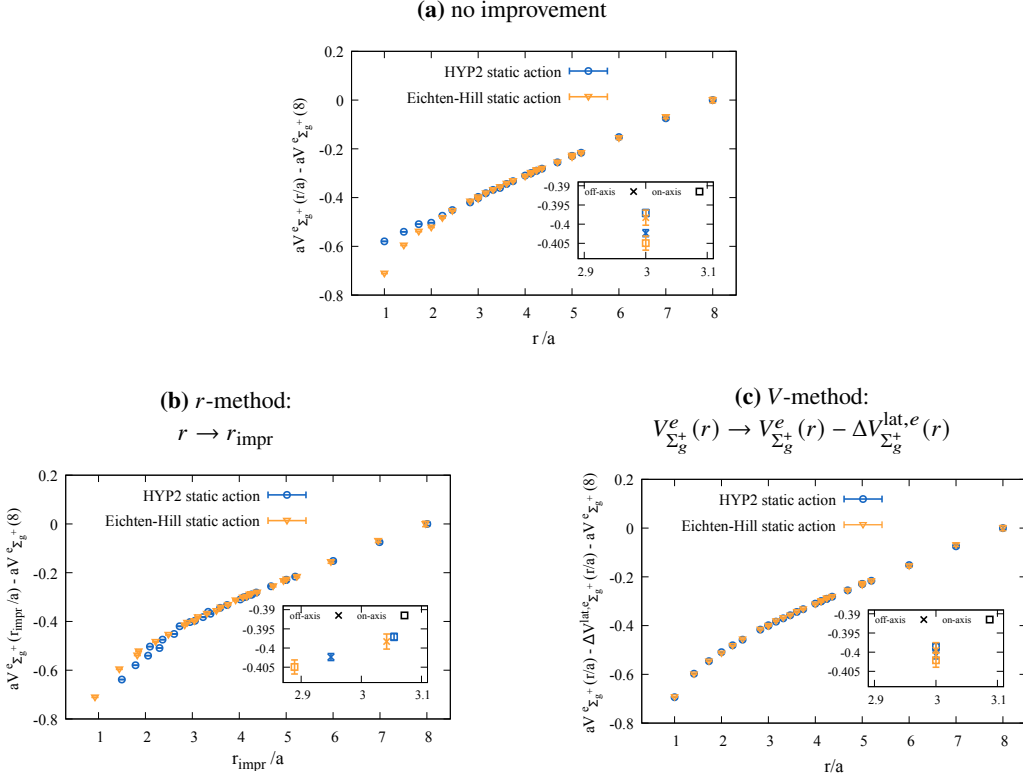


Figure 3: Unimproved and improved SU(2) lattice field theory data for the ordinary static potential at gauge coupling $\beta = 2.40$ for two different discretizations of the static action.

r -dependent term σr . A significant part of the remaining discretization errors can be removed by subtracting the overcorrection term $\bar{\Delta}^{\text{lat}} = \sigma(r - r_{\text{impr}})$ from the r -improved lattice data points for the static potential. σ should be determined by a fit of $V_0 - \alpha/r + \sigma r$ to lattice data points at larger r/a , where discretization errors are negligible. We plan to discuss this in more detail in an upcoming publication. We note that such an additional correction is not necessary for a tree-level improvement of the static force, since the problematic linear term σr in the static potential corresponds to a constant term in the static force which is independent of r .

The alternative V -method [26, 34] corrects the static potential by subtracting the difference between the lattice static potential at tree level, which is proportional to $G(\mathbf{r}/a)/a$, and the continuum static potential at tree-level, which is proportional to $1/r$, from the full lattice static potential, i.e.

$$V_{\Sigma_g^+}^e(r) \rightarrow V_{\Sigma_g^+}^e(r) - \Delta V_{\Sigma_g^+}^{\text{lat},e}(r) = V_{\Sigma_g^+}^e(r) - \alpha' \left(\frac{1}{r} - \frac{G^e(\mathbf{r}/a)}{a} \right). \quad (1)$$

α' is determined by a fit to the unimproved data as discussed in section 5 and is related to the strong coupling constant. The improved data $V_{\Sigma_g^+}^e(r) - \Delta V_{\Sigma_g^+}^{\text{lat},e}(r)$ is presented in Figure 3c. It can be consistently described by a smooth curve and rotational symmetry is restored within statistical errors (see the zoomed plot in Figure 3c).

The important conclusion of this section is that the V -method is clearly superior to the r -method when computing the static potential. On the contrary, for the static force we expect that both methods perform on a similar level.

5. Parametrizations of the hybrid static potentials

To remove lattice discretization errors at tree level of perturbation theory in our SU(3) lattice data, we employ the V -method described in the previous section. We carry out a joint 8-parameter fit to the lattice results for the ordinary static potential from all ensembles $e \in \{A, B, C, D, A^{\text{HYP2}}\}$. The fit function is

$$V_{\Sigma_g^+}^{\text{fit},e}(r) = V_{\Sigma_g^+}(r) + C^e + \Delta V_{\Sigma_g^+}^{\text{lat},e}(r), \quad (2)$$

with the lattice discretization error at tree level, $\Delta V_{\Sigma_g^+}^{\text{lat},e}(r)$, as defined in Eq. (1) (α' is one of the fit parameters), the ensemble-dependent self energy of the static quarks, C^e , and the parametrization of the ordinary static potential,

$$V_{\Sigma_g^+}(r) = -\frac{\alpha}{r} + \sigma r. \quad (3)$$

Eq. (2) is fitted to the lattice data for $r \geq 0.2$ fm. We define the improved lattice data points for the ordinary static potential via

$$\tilde{V}_{\Sigma_g^+}^e(r) = V_{\Sigma_g^+}^e(r) - C^e - \Delta V_{\Sigma_g^+}^{\text{lat},e}(r), \quad (4)$$

where the self energy C^e and the lattice discretization errors at tree level of perturbation theory are subtracted. This improved data is presented together with its parametrization (3) in Figure 4.

The lattice results for the hybrid static potentials Π_u and Σ_u^- from all ensembles can be described consistently by a 10-parameter fit with

$$V_{\Lambda_\eta^\epsilon}^{\text{fit},e}(r) = V_{\Lambda_\eta^\epsilon}(r) + C^e + \Delta V_{\text{hybrid}}^{\text{lat},e}(r) + A_{2,\Lambda_\eta^\epsilon}^{\prime e} a^2 \quad (5)$$

for $r \geq 2a$. For the hybrid static potentials the lattice discretization errors at tree level of perturbation theory are $\Delta V_{\text{hybrid}}^{\text{lat},e}(r) = -\frac{1}{8}\Delta V_{\Sigma_g^+}^{\text{lat},e}(r)$. The parametrizations $V_{\Lambda_\eta^\epsilon}(r)$ with $\Lambda_\eta^\epsilon = \Pi_u, \Sigma_u^-$ are based on a prediction of potential Non-Relativistic QCD for short quark-antiquark separations [12]. They are given by

$$V_{\Pi_u}(r) = \frac{A_1}{r} + A_2 + A_3 r^2 \quad (6)$$

$$V_{\Sigma_u^-}(r) = \frac{A_1}{r} + A_2 + A_3 r^2 + \frac{B_1 r^2}{1 + B_2 r + B_3 r^2} \quad (7)$$

with fit parameters A_1, A_2, A_3 , which are the same for both hybrid static potentials, and an additional term with fit parameters B_1, B_2 and B_3 for the Σ_u^- potential. The term $A_{2,\Lambda_\eta^\epsilon}^{\prime e} a^2$ in Eq. (5) accounts for the discretization error of the constant shift with respect to the ordinary static potential at leading order in the lattice spacing. The fit parameter $A_{2,\Lambda_\eta^\epsilon}^{\prime e}$ with $\Lambda_\eta^\epsilon = \Pi_u$ or Σ_u^- is equal for the ensembles $e \in \{A, B, C, D\}$ and different for the ensemble $e = A^{\text{HYP2}}$.

As before, we define improved data points for the hybrid static potentials by subtracting the self energy C^e , the lattice discretization error at tree level of perturbation theory $\Delta V_{\text{hybrid}}^{\text{lat},e}(r)$ and the lattice discretization error of the constant shift A_2 at leading order in the lattice spacing, $A_{2,\Lambda_\eta^\epsilon}^{\prime e} a^2$, i.e.

$$\tilde{V}_{\Lambda_\eta^\epsilon}^e(r) = V_{\Lambda_\eta^\epsilon}^e(r) - C^e - \Delta V_{\text{hybrid}}^{\text{lat},e}(r) - A_{2,\Lambda_\eta^\epsilon}^{\prime e} a^2. \quad (8)$$

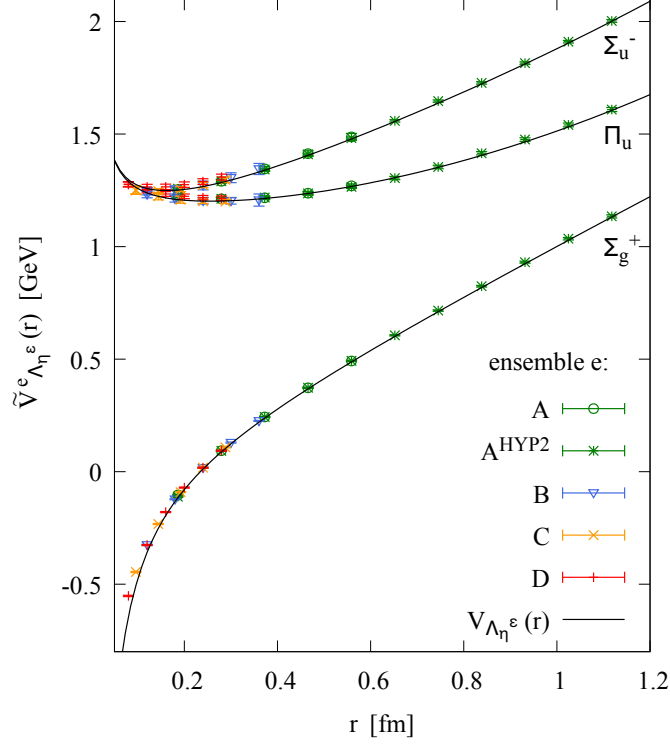


Figure 4: Improved lattice results for the ordinary static potential Σ_g^+ and the hybrid static potentials Π_u and Σ_u^- from the five ensembles $e \in \{A, B, C, D, A^{\text{HYP2}}\}$ and their parametrizations (3), (6) and (7).

The improved lattice data points and the corresponding parametrizations (6) are consistent within statistical errors (see Figure 4) and, thus, seem to represent continuum limit results for hybrid static potentials.

Since we are considering several finer lattice spacings than before, we are able to reach short quark-antiquark separations as small as 0.08 fm. At these small separations the lattice results clearly exhibit the repulsive behavior predicted by perturbation theory and indicate the expected degeneracy for Π_u and Σ_u^- . The parametrizations and improved lattice data points are provided in our related journal publication [25] for straightforward use, e.g. for refined Born-Oppenheimer approaches to predict the spectra of heavy hybrid mesons. The parametrizations provided in this work are expected to change the mass spectra by $\mathcal{O}(10 \dots 45 \text{ MeV})$ compared to parameterizations obtained previously at much coarser lattice spacing (for details see Ref. [25]).

Acknowledgments

We thank Christian Reisinger for providing his multilevel code. We acknowledge interesting and useful discussions with Eric Braaten, Nora Brambilla, Francesco Knechtli, Colin Morningstar, Lasse Müller, Christian Reisinger and Joan Soto.

M.W. acknowledges support by the Heisenberg Programme of the Deutsche Forschungsgemeinschaft (DFG, German Research Foundation) – project number 399217702.

Calculations on the GOETHE-HLR and on the on the FUCHS-CSC high-performance computers of the Frankfurt University were conducted for this research. We thank HPC-Hessen, funded by the State Ministry of Higher Education, Research and the Arts, for programming advice.

References

- [1] S.L. Olsen, T. Skwarnicki and D. Zieminska, *Nonstandard heavy mesons and baryons: Experimental evidence*, *Rev. Mod. Phys.* **90** (2018) 015003 [1708.04012].
- [2] E. Braaten, C. Langmack and D.H. Smith, *Selection Rules for Hadronic Transitions of XYZ Mesons*, *Phys. Rev. Lett.* **112** (2014) 222001 [1401.7351].
- [3] C. Meyer and E. Swanson, *Hybrid Mesons*, *Prog. Part. Nucl. Phys.* **82** (2015) 21 [1502.07276].
- [4] E.S. Swanson, *XYZ States: Theory Overview*, *AIP Conf. Proc.* **1735** (2016) 020013 [1512.04853].
- [5] R.F. Lebed, R.E. Mitchell and E.S. Swanson, *Heavy-Quark QCD Exotica*, *Prog. Part. Nucl. Phys.* **93** (2017) 143 [1610.04528].
- [6] N. Brambilla, S. Eidelman, C. Hanhart, A. Nefediev, C.-P. Shen, C.E. Thomas et al., *The XYZ states: experimental and theoretical status and perspectives*, *Phys. Rept.* **873** (2020) 1 [1907.07583].
- [7] S. Perantonis and C. Michael, *Static potentials and hybrid mesons from pure SU(3) lattice gauge theory*, *Nucl. Phys. B* **347** (1990) 854.
- [8] K. Juge, J. Kuti and C. Morningstar, *Ab initio study of hybrid anti-b g b mesons*, *Phys. Rev. Lett.* **82** (1999) 4400 [hep-ph/9902336].
- [9] P. Guo, A.P. Szczepaniak, G. Galata, A. Vassallo and E. Santopinto, *Heavy quarkonium hybrids from Coulomb gauge QCD*, *Phys. Rev. D* **78** (2008) 056003 [0807.2721].
- [10] E. Braaten, C. Langmack and D.H. Smith, *Born-Oppenheimer Approximation for the XYZ Mesons*, *Phys. Rev. D* **90** (2014) 014044 [1402.0438].
- [11] S. Capitani, O. Philipsen, C. Reisinger, C. Riehl and M. Wagner, *Precision computation of hybrid static potentials in SU(3) lattice gauge theory*, *Phys. Rev. D* **99** (2019) 034502 [1811.11046].
- [12] M. Berwein, N. Brambilla, J. Tarrús Castellà and A. Vairo, *Quarkonium Hybrids with Nonrelativistic Effective Field Theories*, *Phys. Rev. D* **92** (2015) 114019 [1510.04299].
- [13] R. Oncala and J. Soto, *Heavy Quarkonium Hybrids: Spectrum, Decay and Mixing*, *Phys. Rev.* **D96** (2017) 014004 [1702.03900].
- [14] N. Brambilla, W.K. Lai, J. Segovia and J. Tarrús Castellà, *QCD spin effects in the heavy hybrid potentials and spectra*, *Phys. Rev. D* **101** (2020) 054040 [1908.11699].

- [15] S. Perantonis, A. Huntley and C. Michael, *Static potentials from pure $su(2)$ lattice gauge theory*, *Nuclear Physics* **326** (1989) 544.
- [16] C. Michael and S.J. Perantonis, *Potentials and glueballs at large beta in $SU(2)$ pure gauge theory*, *J. Phys. G* **18** (1992) 1725.
- [17] K. Juge, J. Kuti and C. Morningstar, *Glueon excitations of the static quark potential and the hybrid quarkonium spectrum*, *Nucl. Phys. B Proc. Suppl.* **63** (1998) 326 [[hep-lat/9709131](#)].
- [18] K.J. Juge, J. Kuti and C.J. Morningstar, *A Study of hybrid quarkonium using lattice QCD*, *AIP Conf. Proc.* **432** (1998) 136 [[hep-ph/9711451](#)].
- [19] K.J. Juge, J. Kuti and C. Morningstar, *Fine structure of the QCD string spectrum*, *Phys. Rev. Lett.* **90** (2003) 161601 [[hep-lat/0207004](#)].
- [20] G.S. Bali and A. Pineda, *QCD phenomenology of static sources and gluonic excitations at short distances*, *Phys. Rev. D* **69** (2004) 094001 [[hep-ph/0310130](#)].
- [21] K.J. Juge, J. Kuti and C. Morningstar, *Excitations of the static quark anti-quark system in several gauge theories*, in *International Conference on Color Confinement and Hadrons in Quantum Chromodynamics - Confinement 2003*, 2003, DOI [[hep-lat/0312019](#)].
- [22] O. Philipsen, C. Pinke, A. Sciarra and M. Bach, *CL^2 QCD - Lattice QCD based on OpenCL*, *PoS LATTICE2014* (2014) 038 [[1411.5219](#)].
- [23] S. Necco and R. Sommer, *The $N(f) = 0$ heavy quark potential from short to intermediate distances*, *Nucl. Phys. B* **622** (2002) 328 [[hep-lat/0108008](#)].
- [24] M. Lüscher and P. Weisz, *Locality and exponential error reduction in numerical lattice gauge theory*, *JHEP* **09** (2001) 010 [[hep-lat/0108014](#)].
- [25] C. Schlosser and M. Wagner, *Hybrid static potentials in $SU(3)$ lattice gauge theory at small quark-antiquark separations*, *Phys. Rev. D* **105** (2022) 054503 [[2111.00741](#)].
- [26] A. Hasenfratz, R. Hoffmann and F. Knechtli, *The Static potential with hypercubic blocking*, *Nucl. Phys. B Proc. Suppl.* **106** (2002) 418 [[hep-lat/0110168](#)].
- [27] ALPHA collaboration, *Lattice HQET with exponentially improved statistical precision*, *Phys. Lett. B* **581** (2004) 93 [[hep-lat/0307021](#)].
- [28] M. Della Morte, A. Shindler and R. Sommer, *On lattice actions for static quarks*, *JHEP* **08** (2005) 051 [[hep-lat/0506008](#)].
- [29] R. Sommer, *A New way to set the energy scale in lattice gauge theories and its applications to the static force and alpha-s in $SU(2)$ Yang-Mills theory*, *Nucl. Phys. B* **411** (1994) 839 [[hep-lat/9310022](#)].

- [30] TUMQCD collaboration, *Static Energy in (2 + 1 + 1)-Flavor Lattice QCD: Scale Setting and Charm Effects*, [2206.03156](#).
- [31] TUMQCD collaboration, *Determination of the QCD coupling from the static energy and the free energy*, *Phys. Rev. D* **100** (2019) 114511 [[1907.11747](#)].
- [32] A. Bazavov, N. Brambilla, X.G. Tormo, I. P. Petreczky, J. Soto and A. Vairo, *Determination of α_s from the QCD static energy: An update*, *Phys. Rev. D* **90** (2014) 074038 [[1407.8437](#)].
- [33] J. Komijani, P. Petreczky and J.H. Weber, *Strong coupling constant and quark masses from lattice QCD*, *Prog. Part. Nucl. Phys.* **113** (2020) 103788 [[2003.11703](#)].
- [34] C. Michael, *The Running coupling from lattice gauge theory*, *Phys. Lett. B* **283** (1992) 103 [[hep-lat/9205010](#)].